

Hadron production in e^+e^- collisions at *BABAR* and implications for the muon anomalous magnetic moment

Andreas Hafner

Johannes Gutenberg-University Mainz

RadioMCLow
Mainz, 25th September 2012



Institut für Kernphysik

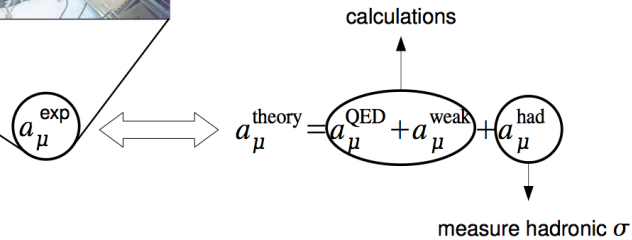


JOHANNES GUTENBERG
UNIVERSITÄT MAINZ

Überblick

- ① Motivation: Muon-Anomaly $(g - 2)_\mu$
- ② Measurement of $\sigma(e^+ e^- \rightarrow \pi^+ \pi^- \pi^+ \pi^-)$
- ③ Measurement of $\sigma(e^+ e^- \rightarrow K^+ K^-)$
- ④ Impact of New Data from BES-III
- ⑤ Summary

The anomalous magnetic moment of the muon $(g - 2)_\mu$



$$e^+e^- \rightarrow \pi^+\pi^-\pi^+\pi^-$$

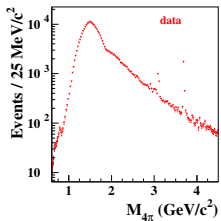
Phys. Rev. D**85**, 112009 (2012), based on 454 fb^{-1}
supersedes our previous publication, based on 89 fb^{-1} of the data:
Phys. Rev. D**71**, 052001 (2005).

Analysis path for $\sigma(e^+e^- \rightarrow \pi^+\pi^-\pi^+\pi^-)$

Invariant 4π mass distribution
after pre-selection

Heart of analysis:
background & efficiency
as function of $M_{4\pi}$

Normalize with Luminosity \mathcal{L}
and radiator function W :
 $\mathcal{L}_{ISR} = \mathcal{L}_{int} \cdot W(s, E_{CM}, \theta_\gamma^*)$



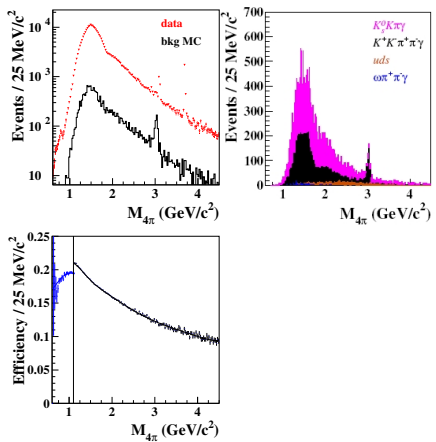
Analysis path for $\sigma(e^+e^- \rightarrow \pi^+\pi^-\pi^+\pi^-)$

Invariant 4π mass distribution
after pre-selection

Heart of analysis:
background & efficiency
as function of $M_{4\pi}$

Normalize with Luminosity \mathcal{L}
and radiator function W :

$$\mathcal{L}_{ISR} = \mathcal{L}_{int} \cdot W(s, E_{CM}, \theta_\gamma^*)$$



Analysis path for $\sigma(e^+e^- \rightarrow \pi^+\pi^-\pi^+\pi^-)$

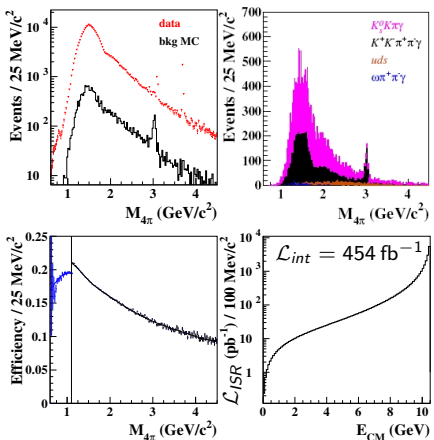
Invariant 4π mass distribution
after pre-selection

Heart of analysis:
background & efficiency
as function of $M_{4\pi}$

Normalize with Luminosity \mathcal{L}
and radiator function W :

$$\mathcal{L}_{ISR} = \mathcal{L}_{int} \cdot W(s, E_{CM}, \theta_\gamma^*)$$

PRD 77, 114005 (2008)



Analysis path for $\sigma(e^+e^- \rightarrow \pi^+\pi^-\pi^+\pi^-)$

Invariant 4π mass distribution
after pre-selection

Heart of analysis:
background & efficiency
as function of $M_{4\pi}$

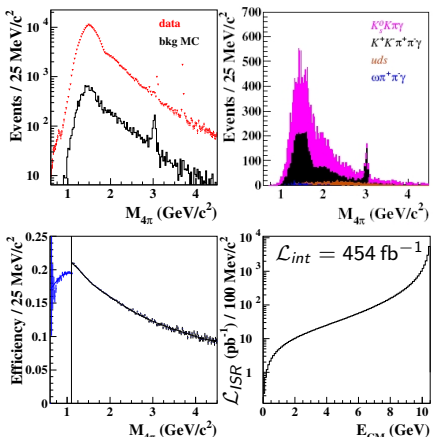
Normalize with Luminosity \mathcal{L}
and radiator function W :

$$\mathcal{L}_{ISR} = \mathcal{L}_{int} \cdot W(s, E_{CM}, \theta_\gamma^*)$$

PRD 77, 114005 (2008)

Cross section:

$$\sigma_{4\pi}(M_{4\pi}) = \frac{dN_{4\pi,\gamma}(M_{4\pi})}{2M_{4\pi} dM_{4\pi}} \cdot \frac{s}{\mathcal{L}_{int} \cdot W(s, E_{CM}, \theta_\gamma^*)} \cdot \frac{1}{\epsilon}$$



Analysis path for $\sigma(e^+e^- \rightarrow \pi^+\pi^-\pi^+\pi^-)$

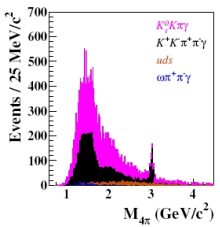
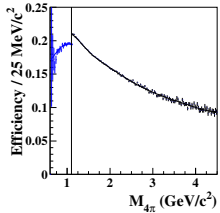
Invariant 4π mass distribution
after pre-selection

Heart of analysis:
background & efficiency
as function of $M_{4\pi}$

Normalize with Luminosity \mathcal{L}
and radiator function W :

$$\mathcal{L}_{ISR} = \mathcal{L}_{int} \cdot W(s, E_{CM}, \theta_\gamma^*)$$

Agreement
btw. simulation
and data?

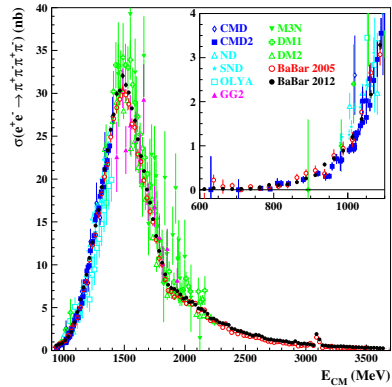
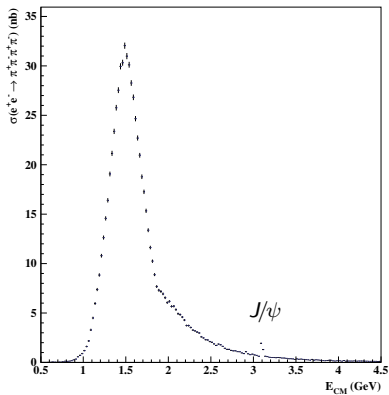


Summary of systematic uncertainties

Systematic uncertainties in %:

$M_{4\pi}$	< 1.1 GeV/c ²	< 2.8 GeV/c ²	< 4.0 GeV/c ²
$K^+K^-\pi^+\pi^-\gamma, K_s^0K^\pm\pi^\mp\gamma$	± 1.0	± 1.0	± 3.0
$\pi^+\pi^-e^+e^-\gamma$	± 3.0	-	-
Continuum background	-	± 0.5	± 1.0
Additional background	± 0.4	± 0.4	± 4.0
Track-rec-efficiency	$+3.0 \pm 1.4$	$+3.0 \pm 1.4$	$+3.0 \pm 1.4$
γ-rec-efficiency	$+1.3 \pm 0.4$	$+1.3 \pm 0.4$	$+1.3 \pm 0.4$
\mathcal{L}	± 1.0	± 1.0	± 1.0
AFK-PHOK-difference	-1.0 ± 0.2	-1.0 ± 0.2	-1.0 ± 0.2
FSR corrections	± 0.5	± 0.2	± 0.1
$\chi^2_{4\pi} < 30$	± 0.3	± 0.3	± 0.3
Global efficiency	± 10.0	± 1.0	± 1.0
Sum	± 10.7	± 2.4	± 5.5

Cross section for $e^+e^- \rightarrow \pi^+\pi^-\pi^+\pi^-$



- Systematic uncertainties
 - 2.4% in peak region (1.1-2.8 GeV)
 - 11% (0.6-1.1 GeV)
 - 5.5% (2.8-4.0 GeV)
- J/ψ visible

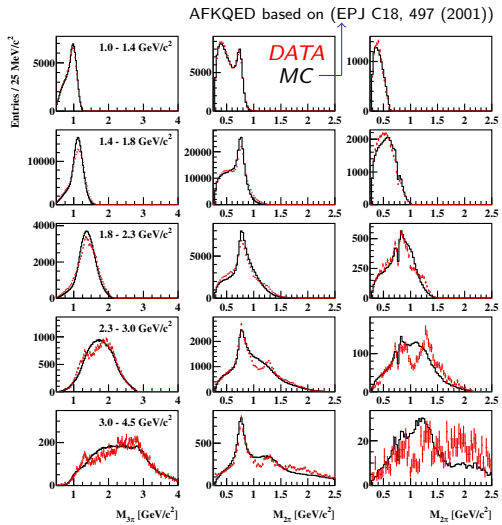
- < 1.4 GeV: agreement with previous **BABAR** results, SND and CMD-2 data
- > 1.4 GeV: highest precision (DM2, 20%)

MC generator issues of this analysis

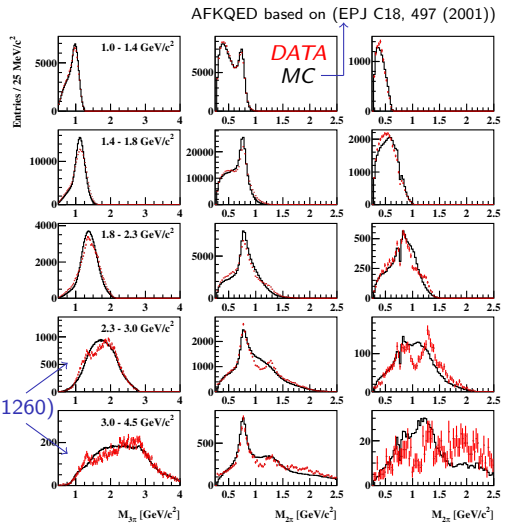
AFKQED vs. PHOKHARA 7

- Influence of internal structure on efficiency
- Simulation of NLO ISR

Internal structure in various E_{CM} energy slices



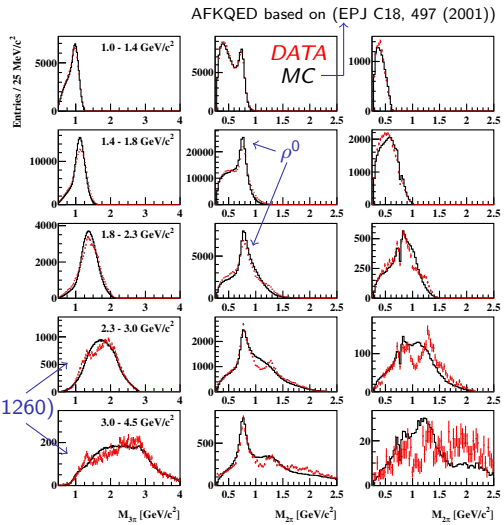
Internal structure in various E_{CM} energy slices



First column (4 entries/event):
 $a_1(1260)$

$a_1(1260)$

Internal structure in various E_{CM} energy slices

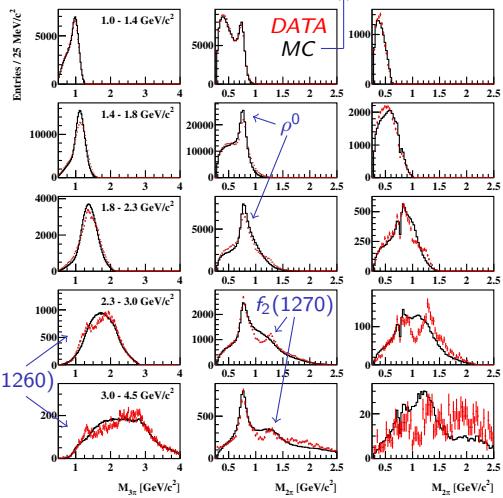


First column (4 entries/event):
 $a_1(1260)$

Second column (4 entries/event):
strong ρ^0 contribution
e.g. for $M_{4\pi} > 1.4 \text{ GeV}/c^2$:
1/4th of entries in ρ^0 peak
 $\rho^0\rho^0$ is forbidden
 $\rightarrow \rho^0$ in each event!

Internal structure in various E_{CM} energy slices

AFKQED based on (EPJ C18, 497 (2001))



First column (4 entries/event):

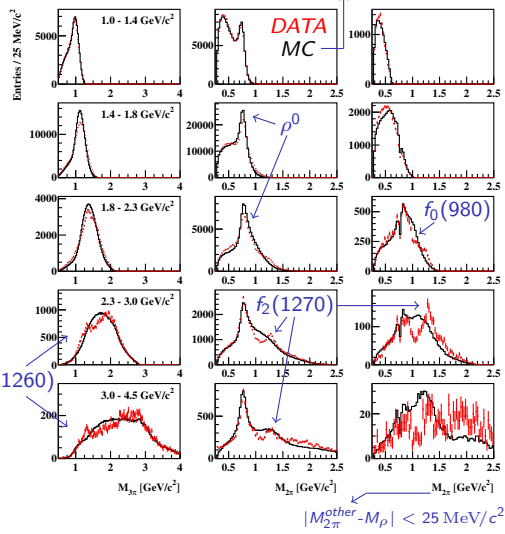
$a_1(1260)$

Second column (4 entries/event):

strong ρ^0 contribution
e.g. for $M_{4\pi} > 1.4 \text{ GeV}/c^2$:
1/4th of entries in ρ^0 peak
 $\rho^0\rho^0$ is forbidden
 $\rightarrow \rho^0$ in each event!

Internal structure in various E_{CM} energy slices

AFKQED based on (EPJ C18, 497 (2001))



First column (4 entries/event):

$a_1(1260)$

Second column (4 entries/event):

strong ρ^0 contribution
e.g. for $M_{4\pi} > 1.4 \text{ GeV}/c^2$:
1/4th of entries in ρ^0 peak
 $\rho^0\rho^0$ is forbidden
 $\rightarrow \rho^0$ in each event!

Third column (1 entry/event):

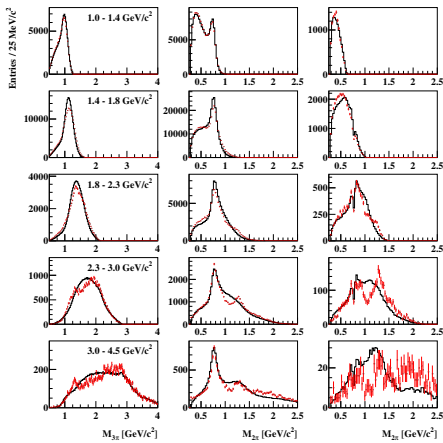
2π lie within ρ^0 mass
 \rightarrow other $\pi^+\pi^-$'s mass plotted

$f_2(1270)$, $a_1(1260)$, $f_0(980) \dots ?$

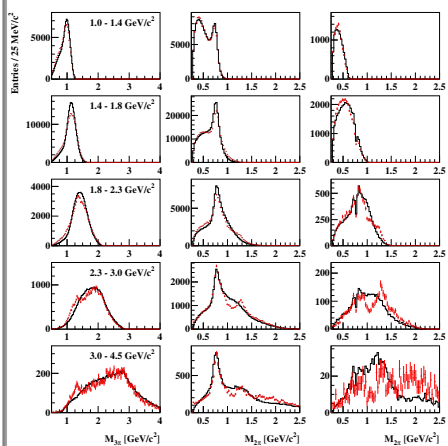
\rightarrow Partial Wave Analysis needed

Internal structure in various E_{CM} energy slices

AFKQED

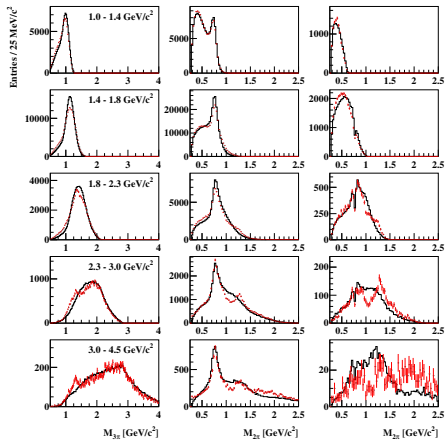


PHOKHARA 5 (standalone)

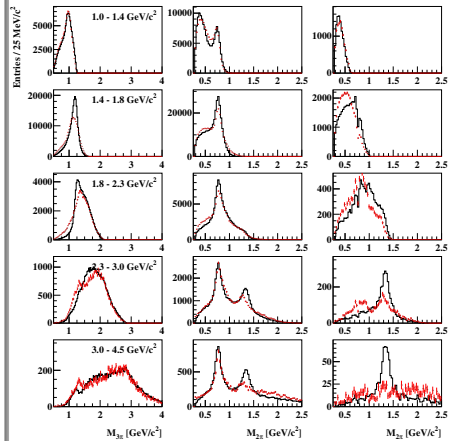


Internal structure in various E_{CM} energy slices

PHOKHARA 5 (standalone)

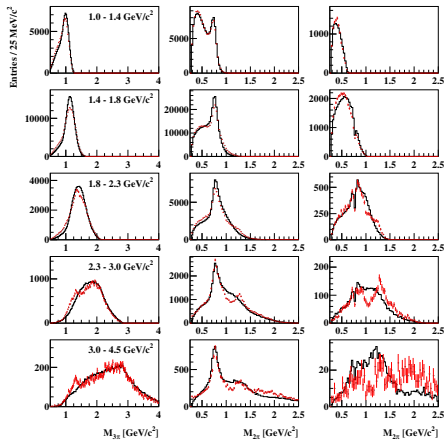


PHOKHARA 7 (standalone)

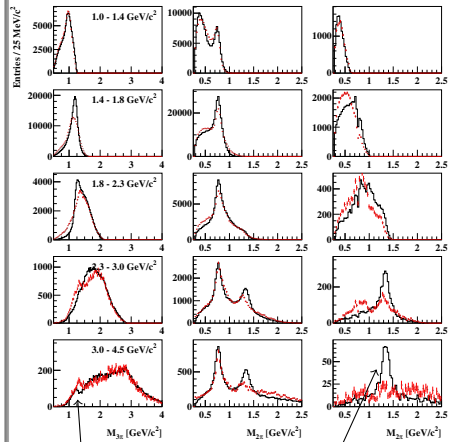


Internal structure in various E_{CM} energy slices

PHOKHARA 5 (standalone)



PHOKHARA 7 (standalone)



$$a_1(M = 1230, \Gamma = 200) \quad f_0(M = 1350, \Gamma = 200)$$

Impact on systematic uncertainty (peak region: 2.4%)

- Intermediate resonances different for AFKQED and PHOKHARA 7:
slightly too less vs. slightly too much
- Acceptance is identical (level of 0.3%):
→ tested via difference between generators
→ tested with angular variation of cuts
- Differences in M_{inv} between data and simulation at high energies!
→ uncertainty in the peak region not affected

NLO ISR

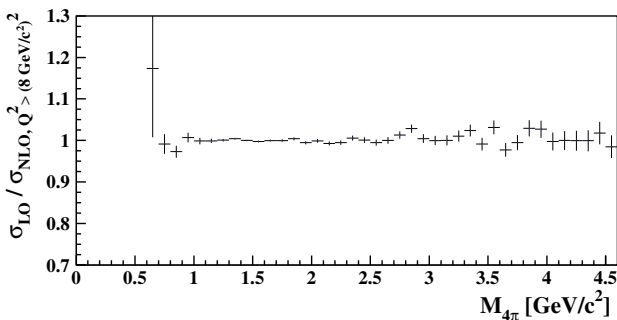
NLO ISR in AFKQED

Quality of radiator function W in AFKQED?

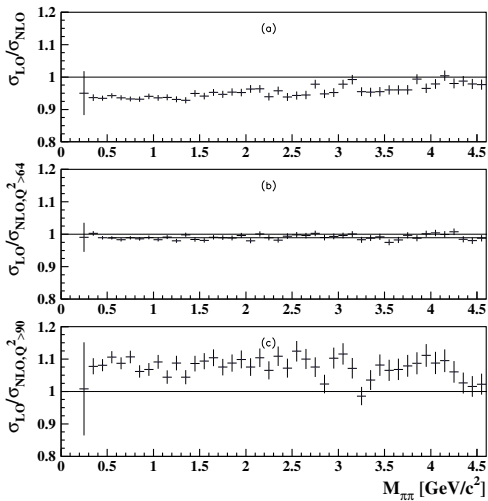
Exclude hard NLO ISR radiation: $Q^2 = (p_{4\pi} + p_{\gamma_{ISR}})^2 > (8 \text{ GeV}/c)^2$

Via the relation: $\frac{d\sigma_{\text{FS},\gamma}(m)}{dm} = \frac{2m}{s} \cdot W(s, x, \theta_\gamma^*) \cdot \sigma_{\text{FS}}(m)$

$$\rightarrow \frac{\sigma_{LO,4\pi\gamma}}{\sigma_{NLO,4\pi\gamma,Q^2>(8 \text{ GeV}/c)^2}} = \frac{W_{LO}}{W_{NLO,4\pi\gamma,Q^2>(8 \text{ GeV}/c)^2}}$$



NLO ISR in Phokhara 7



- Radiator function strongly depends on this requirement
- NLO with $Q^2 > (8 \text{ GeV}/c)^2$ not equivalent to LO radiator function!
→ small additional correction needed
 $(1.0 \pm 0.2\%)$

Impact on $(g - 2)_\mu$

BABAR results:

$$a_\mu^{4\pi, LO}[0.98; 1.8] \text{ GeV} = (13.64 \pm 0.03_{stat} \pm 0.36_{syst}) \cdot 10^{-10} (2.6\%)$$

DEHZ 2003: all results but *BABAR* 2007:

$$a_\mu^{4\pi, LO}[0.98; 1.8] \text{ GeV} = (13.95 \pm 0.90_{exp} \pm 0.23_{rad}) \cdot 10^{-10} (6.7\%)$$

DHMZ 2011: all results but *BABAR* 2012:

$$a_\mu^{4\pi, LO}[0.98; 1.8] \text{ GeV} = (13.35 \pm 0.10_{stat} \pm 0.52_{syst}) \cdot 10^{-10} (4.0\%)$$

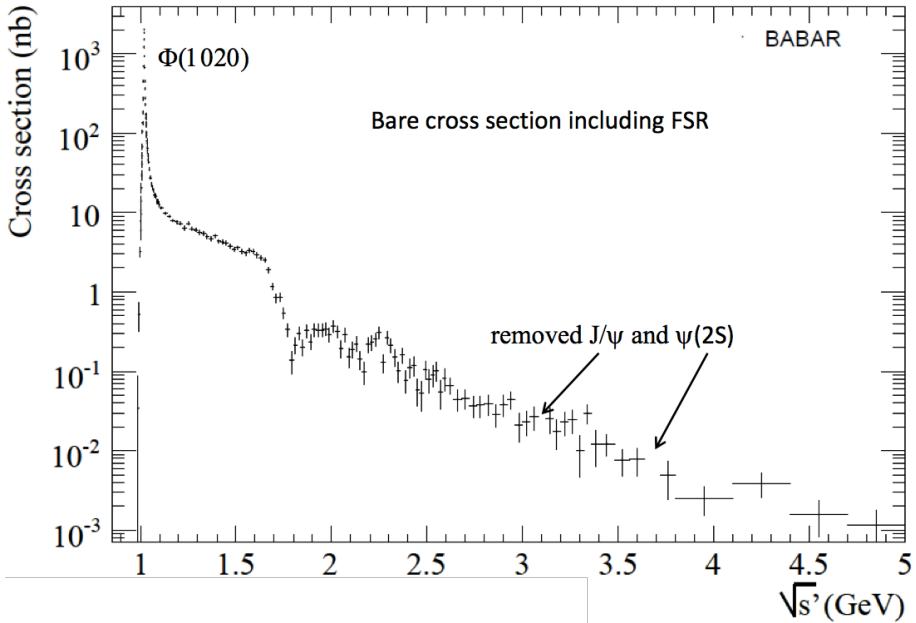
→ *BABAR* more precise than previous world average by a factor of 2.6

$$e^+e^- \rightarrow K^+K^-$$

about to be submitted to Phys. Rev. D, based on 232 fb^{-1}

PRELIMINARY

- Efficiency obtained from full simulation (AfkQed):
→ data/MC corrections of utmost importance:
trigger, tracking, K-ID and mis-ID
- Unfolding bkg-subtracted and data/MC corrected mass spectrum
- PHOKHARA
 - Geometrical acceptance
 - 2ndorder ISR corrections
- ISR effective luminosity from $\mu\mu\gamma(\gamma)$: KK/ $\mu\mu$ ratio



A phenomenological fit to the form factor

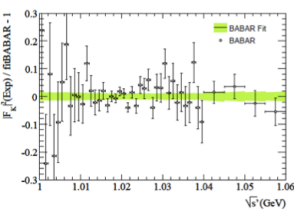
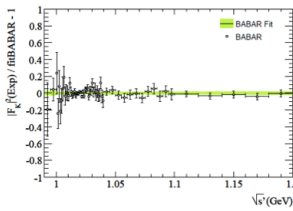
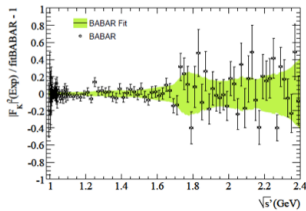
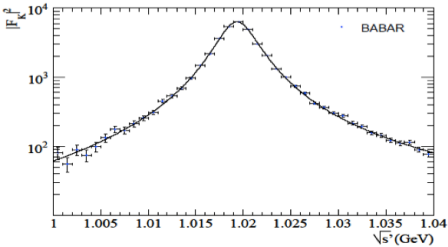
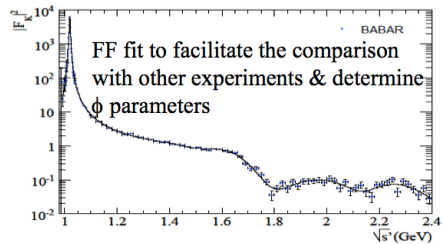
$$\begin{aligned} F_K(s) = & (a_\phi BW_\phi + a_{\phi'} BW_{\phi'} + a_{\phi''} BW_{\phi''}) / 3 \\ & + (a_\rho BW_\rho + a_{\rho'} BW_{\rho'} + a_{\rho''} BW_{\rho''} + a_{\rho'''} BW_{\rho'''}) / 2 \\ & + (a_\omega BW_\omega + a_{\omega'} BW_{\omega'} + a_{\omega''} BW_{\omega''} + a_{\omega'''} BW_{\omega'''}) / 6 \end{aligned}$$

Kuehn et al.

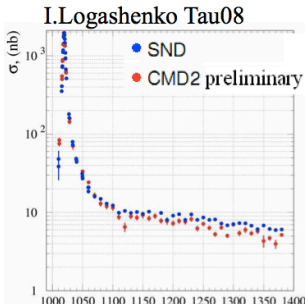
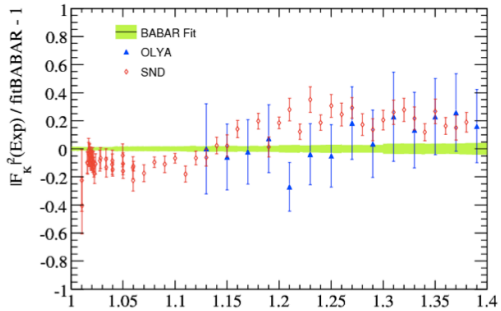
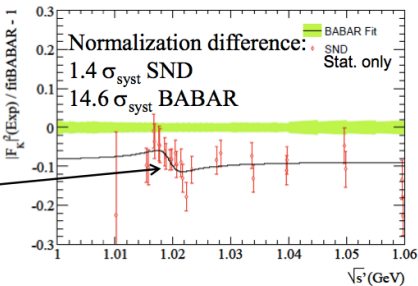
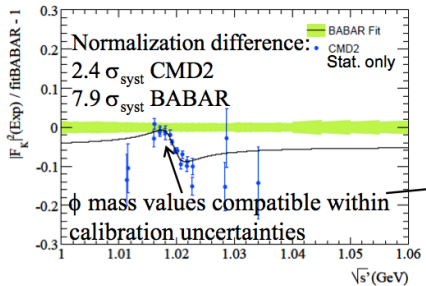
$$a_\phi + a_{\phi'} + a_{\phi''} = 1,$$

$$a_\rho + a_{\rho'} + a_{\rho''} + a_{\rho'''} = 1,$$

$$a_\omega + a_{\omega'} + a_{\omega''} + a_{\omega'''} = 1.$$



Comparison to previous experiments



The Φ parameters

m_Φ and Γ_Φ obtained from the fit of the form factor

BABAR

$$m_\Phi = 1019.51 \pm 0.02 (\pm 0.11) \text{ MeV}$$

$$\Gamma_\Phi = 4.29 \pm 0.04 (\pm 0.07) \text{ MeV}$$

PDG

$$m_\Phi = 1019.455 \pm 0.020 \text{ MeV}$$

$$\Gamma_\Phi = 4.26 \pm 0.04 \text{ MeV}$$

→ good agreement

From integrated Φ peak: $\Gamma_\Phi^{ee} \times \mathcal{B}(\Phi \rightarrow K^+K^-) = \frac{\alpha^2 \beta^3(s, m_K)}{324} \frac{m_\Phi^2}{\Gamma_\Phi} a_\Phi^2 C_{FS}$

BABAR:

$$\Gamma_\Phi^{ee} \times \mathcal{B}(\Phi \rightarrow K^+K^-) = 0.6344 \pm 0.0059_{exp} \pm 0.0028_{fit} \pm 0.0015_{cal} \text{ keV (1.1%)}$$

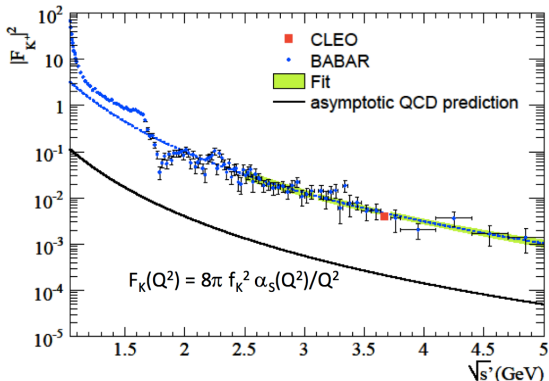
CMD2:

$$\Gamma_\Phi^{ee} \times \mathcal{B}(\Phi \rightarrow K^+K^-) = 0.605 \pm 0.002 \pm 0.013 \text{ keV (2.1%)}$$

Charged kaon form factor at large Q^2

Predictions based on QCD in asymptotic regime (Chernyak, Brodsky-Lepage, Farrar-Jackson)

- Power law: $F_K \sim \alpha_S(Q^2)Q^{-n}$ with $n=2$
→ in good agreement with the data (2.5-5 GeV $n = 2.10 \pm 0.23$)
- HOWEVER: data on $|F_K|^2$ factor ~ 20 above prediction!
- No trend in data up to 25 GeV 2 for approaching the asympt. QCD prediction



Impact on $(g - 2)_\mu$

BABAR results:

$$a_\mu^{K^+K^-, LO} [0.98; 1.8] \text{ GeV} = (22.95 \pm 0.14_{stat} \pm 0.22_{syst}) \cdot 10^{-10} (1.1\%)$$

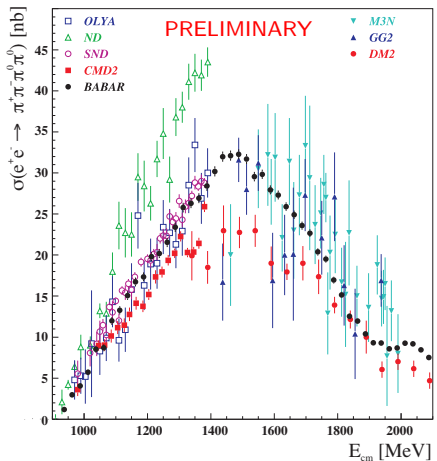
DHMZ 2011: all results before *BABAR*:

$$a_\mu^{K^+K^-, LO} [0.98; 1.8] \text{ GeV} = (21.63 \pm 0.27_{stat} \pm 0.68_{syst}) \cdot 10^{-10} (3.4\%)$$

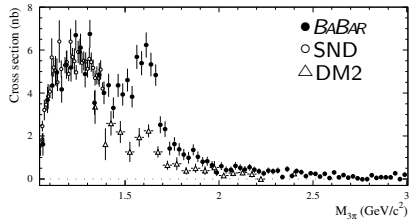
→ *BABAR* more precise than previous world average by a factor of 3

Other high multiplicity channels: $e^+e^- \rightarrow \pi^+\pi^-\pi^0(\pi^0)$

$\pi^+\pi^-\pi^0\pi^0$



$\pi^+\pi^-\pi^0$



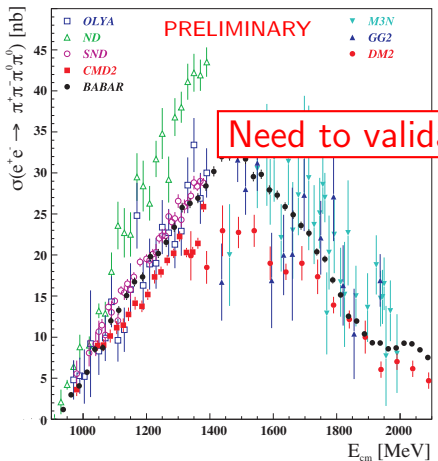
a_μ units in 10^{-10}

Channel	$a_\mu^{had,LO}$	σ_{stat}	σ_{syst}
$\pi^+\pi^-$	507.80	1.22	2.56
$\pi^+\pi^-\pi^0$	46.00	0.42	1.42
$\pi^+\pi^-\pi^0\pi^0$	18.01	0.14	1.24
Total	692.3	1.4	3.9

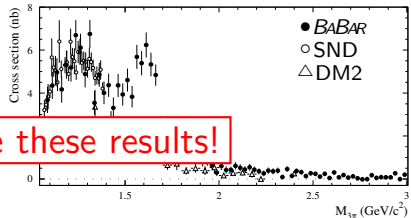
[EPJ C66, 1 (2011).]

Other high multiplicity channels: $e^+e^- \rightarrow \pi^+\pi^-\pi^0(\pi^0)$

$\pi^+\pi^-\pi^0\pi^0$



$\pi^+\pi^-\pi^0$



a_μ units in 10^{-10}

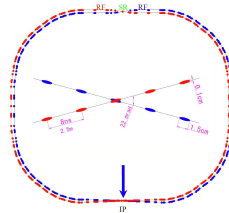
Channel	$a_\mu^{had,LO}$	σ_{stat}	σ_{syst}
$\pi^+\pi^-$	507.80	1.22	2.56
$\pi^+\pi^-\pi^0$	46.00	0.42	1.42
$\pi^+\pi^-\pi^0\pi^0$	18.01	0.14	1.24
Total	692.3	1.4	3.9

[EPJ C66, 1 (2011).]

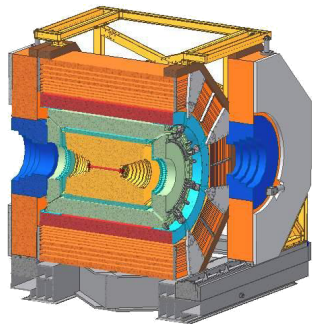
ISR at BES-III

BEPC-II accelerator and BES-III detector

- e^+e^- -collider
- Center-of-Mass energy $\sqrt{s} = 2 - 4.6 \text{ GeV}$
 \Rightarrow below and in the charmonium region
- Luminosity: $0.65 \cdot 10^{33} s^{-1} \text{ cm}^{-2}$



- Multi purpose detector
- Data taking started 2009
- Collected data:
 J/ψ : 1.2 billion
 $\psi(2S)$: 0.5 billion
 ψ'' : 2.9 fb^{-1}
 planned: R-scan [2.0 GeV – 4.5 GeV]
 10 fb^{-1} on ψ''

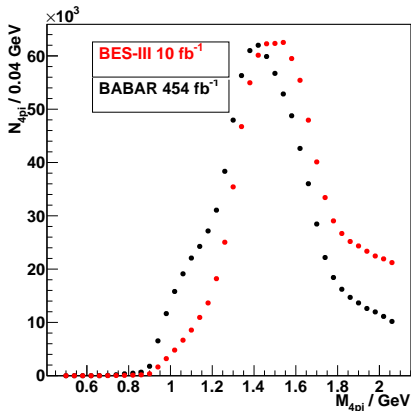


Feasibility study of ISR analyses at BES-III on Ψ''

$$e^+ e^- \rightarrow \pi^+ \pi^- \pi^+ \pi^- \gamma_{ISR}$$

Phokhara event generator (standalone version):

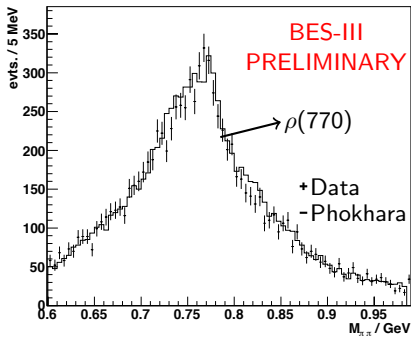
$\rightarrow 10 \text{ fb}^{-1}$ at BES-III correspond to 454 fb^{-1} at *BABAR*



Feasibility study of ISR analyses at BES-III on Ψ''

$e^+e^- \rightarrow \pi^+\pi^-\gamma_{ISR}$:

- Phokhara event generator (within BES simulation framework)
- Data: pre-analysis (tagged) on 400 pb^{-1} performed

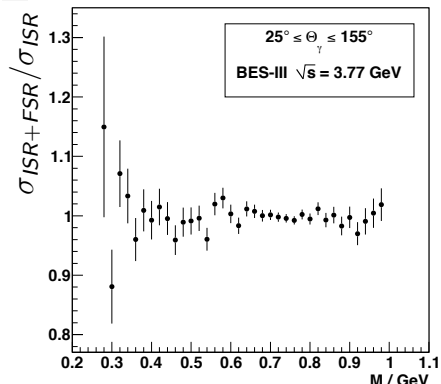
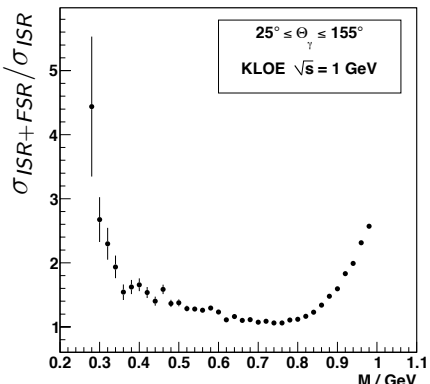


Diploma Thesis Zimmermann

KLOE vs. BES-III vs. *BABAR*

Final State Radiation (FSR)

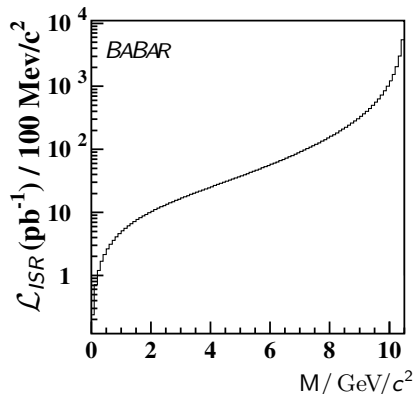
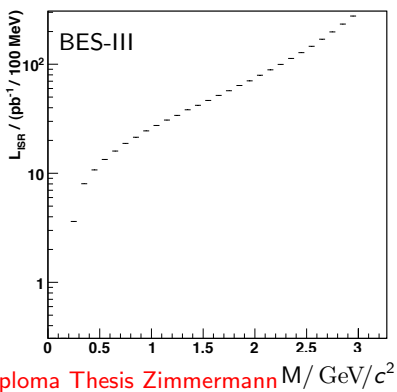
- KLOE runs on $\phi(1020)$ resonance
- Contamination of FSR background at BES-III is much smaller
- FSR description is model dependent



KLOE vs. BES-III vs. *BABAR*

Radiative Return

- *BABAR* runs on $\gamma(4S)$ resonance
- High energetic γ_{ISR} must be radiated $\rightarrow \mathcal{L}_{ISR}$ drops rapidly near ρ

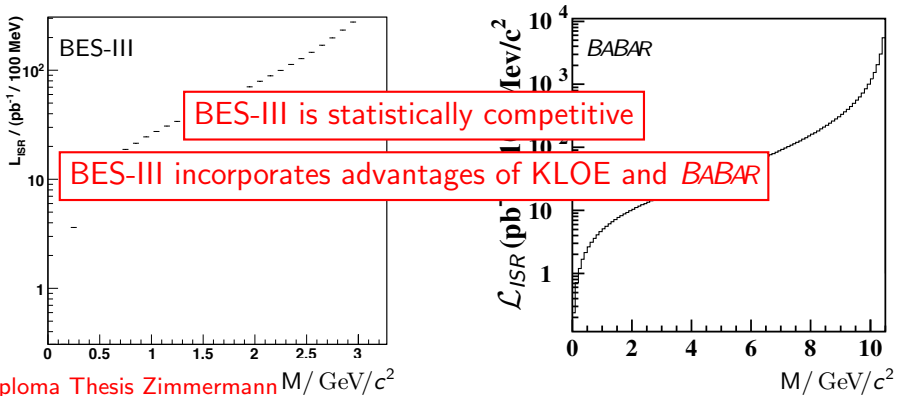


Diploma Thesis Zimmermann M / GeV/c^2

KLOE vs. BES-III vs. *BABAR*

Radiative Return

- *BABAR* runs on $\gamma(4S)$ resonance
- High energetic γ_{ISR} must be radiated $\rightarrow \mathcal{L}_{ISR}$ drops rapidly near ρ



Summary

BABAR

- Measurements from threshold of the invariant mass up to $4.5 \text{ GeV}/c^2$
- Many measurements for the first time with high accuracy
- Hadron spectroscopy
- Important for theoretical predictions of $(g - 2)_\mu$
→ hint for new physics? (3.6σ)

BES-III

- ISR method
 - statistically competitive with *BABAR* and KLOE
 - different systematic uncertainties
- R-Scan important at higher energies

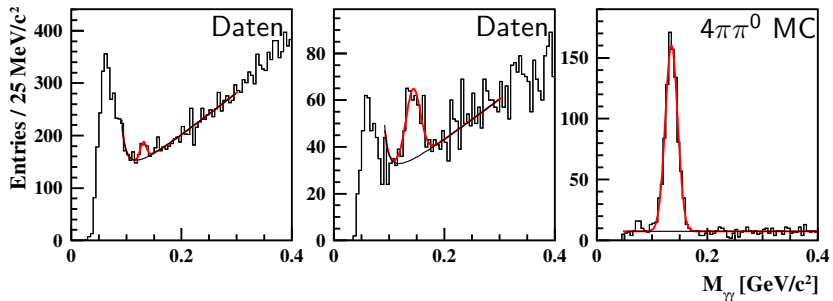
Backup Folien

$$M_{4\pi} > 2.8 \text{ GeV}/c^2$$

$\pi^+\pi^-\pi^+\pi^-\pi^0$ mit $\pi^0 \rightarrow \gamma\gamma \Rightarrow \gamma$ als γ_{ISR} fehlidentifiziert

$$M_{4\pi} < 2.2 \text{ GeV}/c^2$$

$$2.2 \text{ GeV}/c^2 < M_{4\pi} < 4.5 \text{ GeV}/c^2$$



geringer $4\pi\pi^0$ Anteil

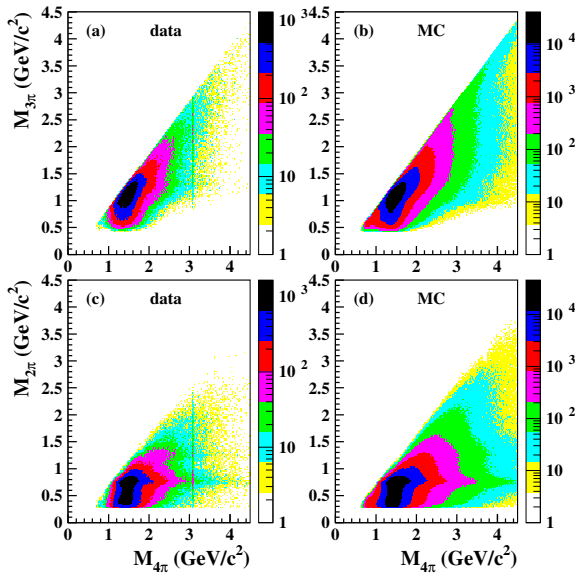
Untergrund abschätzen

hoher $4\pi\pi^0$ Anteil

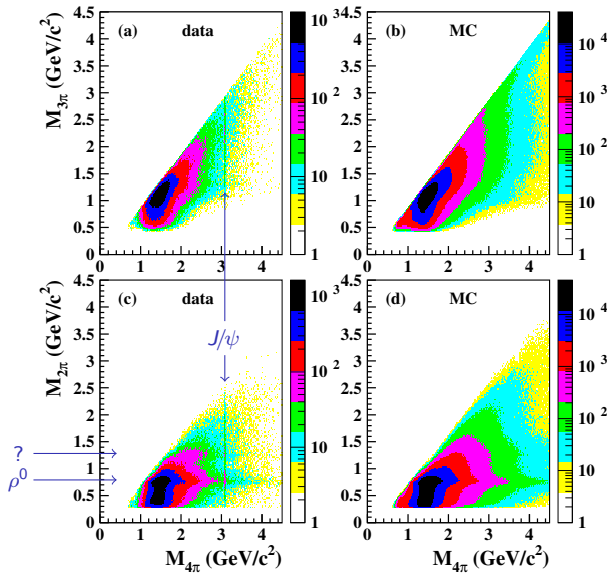
Anzahl $4\pi\pi^0$ Ereignisse
in Daten bestimmen

$4\pi\pi^0$ Simulation
skalieren

Substrukturen in verschiedenen $M_{4\pi}$ Regionen



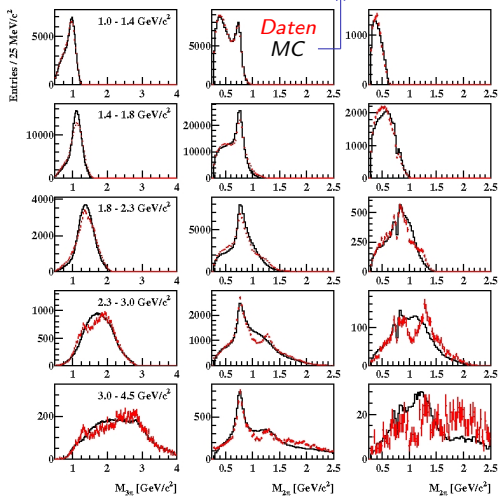
Substrukturen in verschiedenen $M_{4\pi}$ Regionen



Substrukturen in verschiedenen $M_{4\pi}$ Regionen

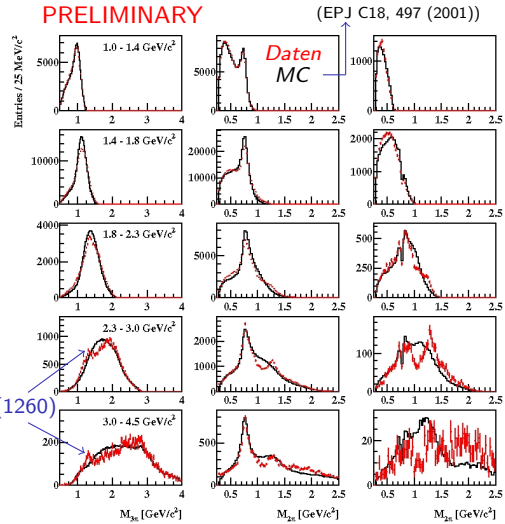
PRELIMINARY

(EPJ C18, 497 (2001))



Substrukturen in verschiedenen $M_{4\pi}$ Regionen

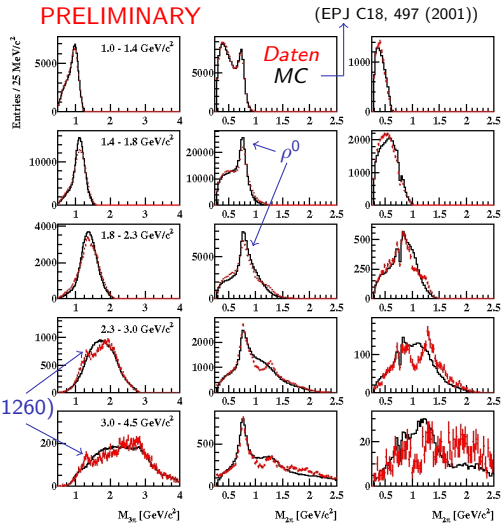
PRELIMINARY



1. Spalte (4 Einträge/Ereignis):
 $a_1(1260)$

Substrukturen in verschiedenen $M_{4\pi}$ Regionen

PRELIMINARY



1. Spalte (4 Einträge/Ereignis):

$a_1(1260)$

2. Spalte (4 Einträge/Ereignis):

großer ρ^0 Beitrag

für $M_{4\pi} > 1.4 \text{ GeV}/c^2$:

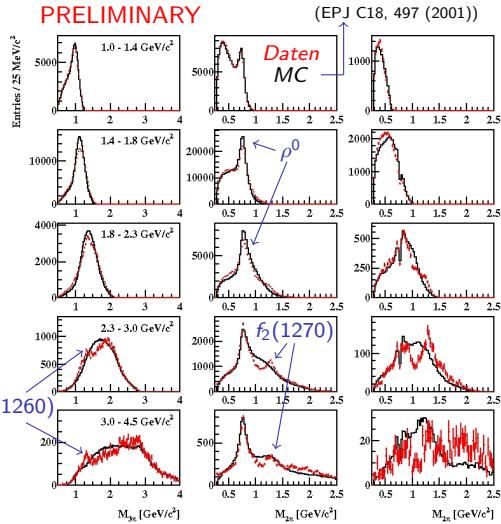
25% der Einträge im ρ^0 Peak

$\rho^0 \rho^0$ ist verboten

$\Rightarrow \rho^0$ in jedem Ereignis!

Substrukturen in verschiedenen $M_{4\pi}$ Regionen

PRELIMINARY



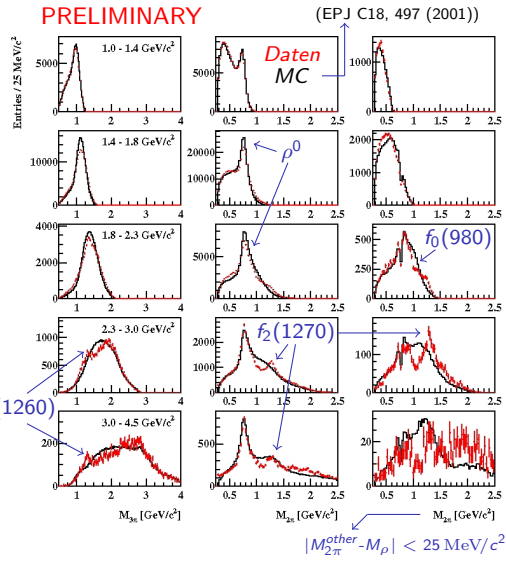
(EPJ C18, 497 (2001))

1. Spalte (4 Einträge/Ereignis):
 $a_1(1260)$

2. Spalte (4 Einträge/Ereignis):
großer ρ^0 Beitrag
für $M_{4\pi} > 1.4 \text{ GeV}/c^2$:
25% der Einträge im ρ^0 Peak
 $\rho^0 \rho^0$ ist verboten
 $\Rightarrow \rho^0$ in jedem Ereignis!

Substrukturen in verschiedenen $M_{4\pi}$ Regionen

PRELIMINARY



1. Spalte (4 Einträge/Ereignis):

$a_1(1260)$

2. Spalte (4 Einträge/Ereignis):

großer ρ^0 Beitrag

für $M_{4\pi} > 1.4 \text{ GeV}/c^2$:

25% der Einträge im ρ^0 Peak

$\rho^0 \rho^0$ ist verboten

$\Rightarrow \rho^0$ in jedem Ereignis!

3. Spalte (1 Eintrag/Ereignis):

2π innerhalb ρ^0 Masse

\Rightarrow andere $\pi^+ \pi^-$ -Masse eingetragen

$f_2(1270)$, $a_1(1260)$, $f_0(980) \dots ?$

\Rightarrow PWA nötig